Since January 2020 Elsevier has created a COVID-19 resource centre with free information in English and Mandarin on the novel coronavirus COVID-19. The COVID-19 resource centre is hosted on Elsevier Connect, the company's public news and information website.

Available online at www.sciencedirect.com
ScienceDirect
Biochemical and Biophysical Research Communications 348 (2006) 916–922
BBRC
www.elsevier.com/locate/ybbrc

Structural characterization of Mumps virus fusion protein core

Yueyong Liu [a,1], Yanhui Xu [b,1], Zhiyong Lou [b,1], Jieqing Zhu [a], Xuebo Hu [a], George F. Gao [a], Bingsheng Qiu [a,*], Zihe Rao [b,*], Po Tien [a,*]

[a] *Institute of Microbiology, Chinese Academy of Sciences, Beijing 100080, China*
[b] *Laboratory of Structural Biology, Tsinghua University, Beijing 100084, China*

Received 19 July 2006
Available online 4 August 2006

Abstract

The fusion proteins of enveloped viruses mediating the fusion between the viral and cellular membranes comprise two discontinuous heptad repeat (HR) domains located at the ectodomain of the enveloped glycoproteins. The crystal structure of the fusion protein core of Mumps virus (MuV) was determined at 2.2 Å resolution. The complex is a six-helix bundle in which three HR1 peptides form a central highly hydrophobic coiled-coil and three HR2 peptides pack against the hydrophobic grooves on the surface of central coiled-coil in an oblique antiparallel manner. Fusion core of MuV, like those of simian virus 5 and human respiratory syncytium virus, forms typical 3-4-4-4-3 spacing. The similar charecterization in HR1 regions, as well as the existence of O–X–O motif in extended regions of HR2 helix, suggests a basic rule for the formation of the fusion core of viral fusion proteins.

Keywords: Mumps virus; Fusion protein; Heptad repeat domains; Fusion core; Crystal structure

Mumps virus (MuV) belongs to genus *Rubulavirus*, family *Paramyxoviridae*, and can infect the glands, the central nervous system, the respiratory tract, and possibly also muscle and connective tissue [1]. Both surface glycoproteins, the hemagglutinin neuraminidase protein (HN) and the fusion (F) protein, are needed to effectuate an efficient viral fusion process mediated by Mumps virus [2]. MuV fusion protein shares many common features with those of other viral enveloped glycoproteins, including the hemagglutinin (HA) protein of influenza virus, gp160 of human immunodeficiency virus (HIV-1) and simian immunodeficiency virus (SIV), glycoprotein of Ebola virus, and fusion protein of paramyxovirus [3,4]. The fusion protein of MuV is synthesized as a precursor protein molecule (F0) which is cleaved in vivo by a host cell protease to yield the active F protein [5]. The mature F protein is composed of two disulfide-linked polypeptides, the distal subunit F2 and the transmembrane subunit F1, of unequal size (Fig. 1A). A highly hydrophobic conserved domain in the membrane-anchored subunit (F1), termed the fusion peptide, is considered to participate in the membrane fusion event as it would insert into the targeted cellular membrane.

The regions following the fusion peptide have a 4-3 heptad repeat (HR) of conserved hydrophobic residues for class I viral fusion proteins. The first heptad repeat, termed the HR1, is followed by a long spacer domain (in some viruses it is short) and a second heptad repeat, termed the HR2, followed by another short spacer and the transmembrane (TM) anchor (Fig. 1A). Previous studies of HA2 [6], HIV-1/SIV gp41 [7–13], Ebola virus GP2 [14,15], Simian virus 5 (SV5) F1 [16], and MHV fusion core [17] indicate that these heptad repeat regions form six-helix bundles which are considered as fusion core of these glycoproteins in a post-fusion form. Three HR1 peptides form hydrophobic central coiled-coil and three HR2 helices pack against the central core in an oblique antiparallel manner [3].

* Corresponding authors. Fax: +86 10 62550162.
E-mail addresses: Qiubs@sun.im.ac.cn (B. Qiu), raozh@xtal.tsinghua.edu.cn (Z. Rao), tienpo@sun.im.ac.cn (P. Tien).
[1] These authors contributed equally to this work.

0006-291X/$ - see front matter © 2006 Elsevier Inc. All rights reserved.
doi:10.1016/j.bbrc.2006.07.168

Previous biochemical studies indicate that the viral fusion proteins undergo a series of conformational changes when activated [4,18]. Earlier studies on HA of influenza and gp41 of HIV-1 led to a model for membrane fusion mediated by envelope glycoproteins [3]. In this model, the N (HR1) and C (HR2) peptides of HIV gp41 come together and form a highly stable coiled-coil aligning the vial and cellular membranes juxtaposition, facilitating membrane fusion, and viral entry [19].

Our recent studies of HR1 and HR2 regions in MuV fusion protein have shown that its HR1 and HR2 also form a stable six-helix bundle, suggesting a common core architecture similar to those of other viral fusion protein [20]. These methods have been successfully used in the biochemical and structural analysis of several other viral fusion protein core, including SARS-CoV [21,22], MHV [17], Newcastle disease virus [23,24], Nipah virus, and Hendra virus [25]. Here, we report the determination of crystal structure of MuV fusion core to 2.2 Å resolution by X-ray crystallography. The structure confirms the similarity between the MuV and other viral fusion proteins, indicating a similar mechanism for viral fusion mediated by Mumps virus. The C terminus of HR1 peptide shows a 3-4-4-4-3 spacing, which is conserved in known SV5 F and HRSV F structure, suggesting the conserved fusion function and mode in family *Paramyxoviridae*. This structure also adds the repertoire of fusion cores of viral fusion proteins, providing more structural information for understanding of formation of post-fusion state of viral fusion proteins.

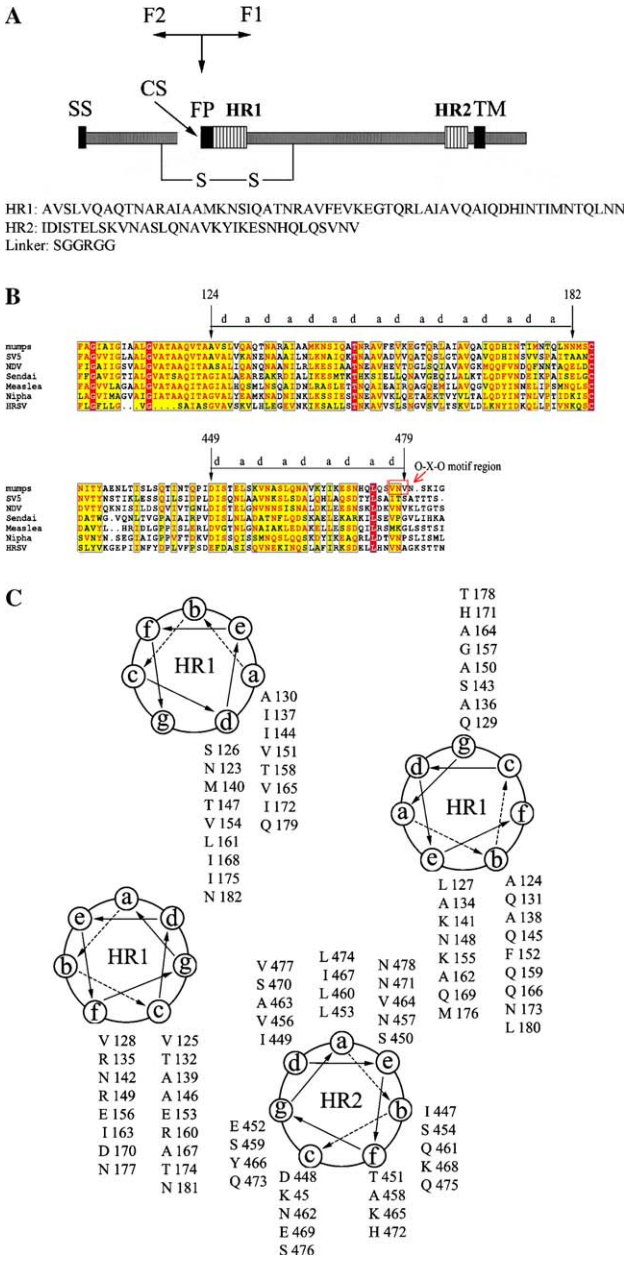

Fig. 1. Construction and sequence characterization of the MuV F protein 2-helix. (A) Schematic diagram of MuV F protein 2-helix constructs. F1 and F2 are formed after proteolytic cleavage (vertical arrow) and covalently linked by a disulfide bond. The fusion protein has an N-terminal signal sequence (SS) and a transmembrane domain (TM) adjacent to the C terminus. F1 contains two HR (heptad repeat) regions (hatched bars), termed HR1 and HR2, as indicated. FP (hatched bars) is an N-terminal fusion peptide followed by HR1 region. MuV 2-helix was constructed as a single polypeptide by linking two HR regions with a six-residue linker (SGGRGG). The amino-acid sequences for HR1 and HR2 used in this study were shown under schematic diagram. (B) Sequence alignment of paramyxovirus spike protein HR1 and HR2 regions. The identical and similar amino acids were indicated in red and yellow background, respectively. Letters above the sequence indicate the predicted hydrophobic heptad repeat a and d residues, which are highly conserved. O–X–O motif of Mumps virus HR2 region is shown in red box. (C) Helical wheel representation of HR1 and HR2. Three HR1 helices and one HR2 helix are represented as helical wheel projections in a top view form. The three central HR1 helices form a central trimic coiled-coil with the hydrophobic interaction of residues in the a and d positions. The three HR2 helices pack against grooves on the surface of the central coiled-coil, aligning residues at the a and d positions in HR2 and the residues at the e and g positions in HR1. These residues, mediating the interactions between HR1 and HR2, are always hydrophobic and highly conserved (B). (For interpretation of the references to color in this figure legend, the reader is referred to the web version of this paper.)

Materials and methods

Expression, purification, and crystallization. The construction, expression, purification, and biochemical studies of MuV fusion core protein was described previously [20]. The purified MuV fusion core protein were dialyzed against 10 mM Tris, pH8.0, 10 mM NaCl, and concentrated to 20 mg ml^{-1}. Crystallization was performed by the hanging-drop vapor-diffusion method at 291 K. One microliter protein solution was mixed with 1 μl reservoir solution and the mixture was equilibrated against 200 μl reservoir solution at 291 K. Crystallization conditions were screened using Crystal Screen reagent kits (Hampton Research). Crystals with good quality can be obtained in 15% PEG800, 0.5 M lithium sulfate in 2 weeks.

Data collection and processing. Data collection of MuV fusion core was performed in-house on a Rigaku RU2000 rotating-copper-anode X-ray generator operated at 48 kV and 98 mA (CuKα; $\lambda = 1.5418$ Å) with a MAR 345 image-plate detector. The crystal was mounted on nylon loops and flash-cooled in cold nitrogen-gas stream at 100 K using an Oxford Cryosystems with reservoir solution as the cryoprotectant. Data were indexed, integrated, and scaled using DENZO and SCALEPACK programs [26].

Table 1
Data collection and final refinement statistics of MuV fusion core structure

Data collection statistics	
Molecule	MuV 2-helix
Space group	C2
Unit cell parameters	$a = 161.2$ Å $b = 60.8$ Å $c = 40.1$ Å $\beta = 98.4°$
Wavelength (Å)	1.5418
Resolution limit (Å)	2.2
Observed reflections	79655
Unique reflections	18557
Completeness (%)	96.3(94.2)
$\langle I/\sigma(I)\rangle$	9.9(3.1)
Rmerge[a] (%)	12.2(48.4)
Final refinement statistics	
Rwork[b] (%)	23.9
Rfree[c] (%)	27.8
Resolution range (Å)	50–2.2
Average B value (Å^2)	34.7
Number of reflections in working set	16332
Number of reflections in test set	851
rmsd bonds[d] (Å)	0.006
rmsd angles (°)	0.95

Numbers in parentheses correspond to the highest resolution shell.
[a] Rmerge $= \sum h \sum I |Iih - \langle Ih\rangle| / \sum h \sum I \langle Ih\rangle$, where $\langle Ih\rangle$ is the mean of the observations Iih of reflection h.
[b] Rwork $= \sum(||F_{obs}| - F_{calc}||)/\sum|F_{obs}|$.
[c] Rfree is the R factor for a subset (5%) of reflections that was selected prior refinement calculations and not included in the refinement.
[d] r.m.s.d.: root mean square deviation from ideal geometry.

Phase determination and model refinement. The structure of MuV fusion core was solved by molecular replacement with the program CNS [27]. A model derived from the SV5F N1/C1 trimer [16] was used as a search model. The MuV fusion core trimer molecules were built into the electron density map using the program O [28]. After several cycles of manual building and refinement using the programs O [28] and CNS [27] without non-crystallographic restrain, the structure was subsequently refined to a final resolution of 2.2 Å with an R-value of 23.5% and free-R-value of 27.9%. The quality of the structure was verified by PROCHECK [29]. No residue was in disallowed regions and 98% residues were in most-preferred regions of the Ramachandran plot. The data collection statistics and the structure refinement statistics are summarized in Table 1. The figures were generated with the programs GRASP [30], SPDBViewer [31], and MOLSCRIPT [32].

Protein Data Bank Accession numbers. The coordinates and the structure factors have been deposited in the RCSB Protein Data Bank with Accession code 2FYZ.

Results and discussion

Structure Determination

Two regions encompassing the N-terminal and C-terminal heptad repeats of MuV fusion protein assemble into a stable trimer of heterodimers [20]. The HR1 region consists of residues 124–184 and the HR2 of residues 447–486 of the MuV F protein sequence (GenBank Accession No. NP_054711.1) (Fig. 1A). The fusion core of MuV fusion protein was prepared as a single chain by linking the HR1 and HR2 domains via a six amino-acid linker (SGGRGG, single amino-acid abbreviation used here). The constructs and the encoded proteins were also called 2-helix (Fig. 1A). The preparation and characterization of the 2-helix proteins have been reported earlier [20]. The MuV 2-helix forms crystals which have unit-cell parameters $a = 161.2$, $b = 60.8$, $c = 40.1$ Å, $\alpha = 90°$, $\beta = 98.4°$, $\gamma = 90°$, and belongs to space group C2. The crystals contain three HR1/HR2 2-helix and 378 water molecules per asymmetric unit and the diffraction pattern extends to 2.2 Å resolution [33].

The crystal structure of the MuV 2-helix was solved by molecular replacement from a single crystal of the protein. A model derived from the SV5 fusion core trimer was used as a search model. The model was further improved by cycles of manual building and refinement using the programs O [28] and CNS [27]. The structure was subsequently refined to a final resolution of 2.2 Å with R-value of 23.5% and free-R-value of 27.9%. No residues were in disallowed regions, and 98% were in the most favored regions of the Ramachandran plot. The data collection statistics and final model statistics are summarized in Table 1.

Description of the structure

In the three-dimensional structure of the MuV 2-helix, the fusion core has a rod-shaped structure approximately 90 Å in length and a maximum diameter of 28 Å. The complex is a six-helix bundle (trimer of heterodimer), similar to other viral fusion core structures. The center of this bundle consists of a parallel trimeric coiled-coil of three HR1 helices which are packed by three HR2 helices in an oblique antiparallel manner (Fig. 2A and B). The rmsd between each pair of HR1 and HR2 are 1.13 and 1.21 Å, respectively. The N terminus of HR1 and the C terminus of HR2 are located to the same end of the six-helix bundle, presumably placing the fusion peptides inserted into the cellular membrane and transmembrane domains in viral membrane close together. Several residues in linker (SGGRGG) and several terminal residues at the C terminus of HR1 regions were disordered and could not be traced in electron density map. Here, we focused our structural analysis on the well-defined regions, including residues 124–179 in HR1 region and residues 449–475 in HR2 region.

Residues 124–179 of HR1 region fold into a 16-turn α-helix stretching the entire length of the coiled-coil. As in other naturally occurring coiled-coil of the fusion core, the residues at the a and d positions in HR1 region are predominantly hydrophobic, although occasional polar residues are also observed in these positions (Fig. 1B and C). A sequence alignment of MuV and several typical paramyxoviruses fusion proteins shows that the residues at these heptad repeat positions are highly conserved (Fig. 1B).

Residues 449–475 of HR2 region form a 7-turn amphipathic α-helix. Each HR2 helix packs against the long grooves on the surface of central coiled-coil. There is no

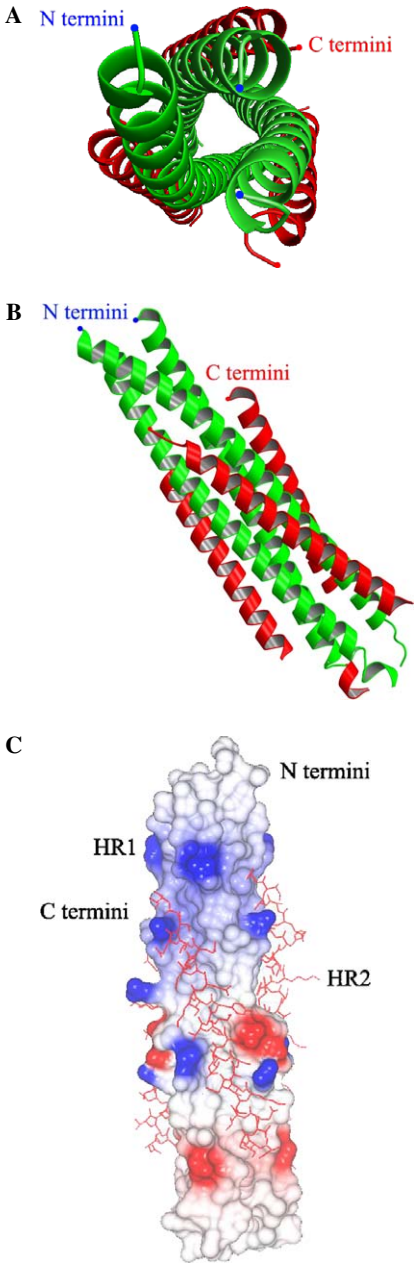

Fig. 2. Overall views of the MuV fusion core structure. (A) Top view of the MuV fusion core structure showing the threefold axis of the trimer. (B) Side view of the MuV fusion core structure showing the six-helix bundle. (C) Electronic potential surface map showing three HR2 helices (red sticks) pack against the hydrophobic grooves of HR1 (blue represents negative charge; red represents positive charge) in an oblique antiparallel manner. (For interpretation of the references to color in this figure legend, the reader is referred to the web version of this paper.)

interaction between individual HR2 helix (Fig. 2A and B). The C terminus of HR2 ends with Q475, aligning with A138 which is also the N terminus of the HR1. The N terminus of HR2 starts with I449, aligning with Q169 of HR1.

Interactions between the HR1 and HR2

Three HR2 helices pack obliquely against the hydrophobic grooves of the central coiled-coil trimer in an antiparallel orientation. The HR2 peptides interact with HR1 peptides mainly through hydrophobic residues and hydrophobic grooves on the surface of central coiled-coil (Fig. 2C). Sequence alignment between MuV and other paramyxoviruses fusion proteins shows that the residues contribute to the HR1/HR2 interaction (residues at the e and g positions in HR1, residues at the a and d positions in HR2) are highly conserved (Fig. 1B).

This pattern of sequence conservation can also be shown on a helical wheel representation of three HR1 helices and one HR2 helix (Fig. 1C). In this diagram, residues at the a and d positions in HR2 region align with residues at the e and g positions in HR1, mainly through hydrophobic interaction with the grooves on the surface of central coiled-coil. Sequence alignment between MuV and SV5 fusion protein shows that 7 out of 16 nonconservative changes exist at the e and g positions in HR1, and only one change (I–L) at the a and d positions in HR2. In contrast, 15 out of 26 nonconservative changes occur at the outside f, b, and c positions in HR1, and 18 out of 22 nonconservative changes occur at positions other than a and d positions in HR2 (Fig. 1B).

Comparison with SV5 F1 fusion core and that of other viral fusion proteins

Among paramyxovirus fusion proteins, only the structures of the SV5 and hRSV fusion core have been determined [16,34]. Here, we focus our structural comparison on MuV F and SV5 F since the fusion core structures of hRSV and SV5 share significant similarity (Fig. 3A and B). MuV fusion core structure has a similar conformation with SV5 F1 and the two structures can be superposed with an RMS deviation of 0.89 Å between all Cα atoms. Although MuV and SV5 fusion cores are very similar in the whole conformation, they also have some significant differences.

In SV5 F structure, the last two heptad repeats of the nine in HR1 region exhibit a skip or increase in spacing [16]. The side chains of I172, V176, I180, and A183 in the C terminus of HR1 peptide produce a 3-4-4-4-3 spacing rather than the expected 3-4-3-4-3. This skip was predicated to be conserved in paramyxovirus and also found in hRSV F structure [34]. In MuV fusion core structure, all the heptad repeats also exhibit the typical 3-4-4-4-3 spacing predicated by LearnCoil-VMF program [35]. In the core structure studied here, I175 faces the outside of the trimer and holds d position in heptad repeats of HR1 region, while M176 at the e position faces the center of the central coiled-coil (Fig. 4A). Sequence alignment shows that residues in the same position in other paramyxovirus fusion proteins as I175 in MuV F are almost all hydrophilic (Val in SV5 F) and the next residues are all hydrophobic and highly conserved (Fig. 4B). This arrangement will lead to increase in spacing that will make the central coiled-coil more stable within the hydrophobic interaction and the outer side of the fusion core more hydrophilic in solution.

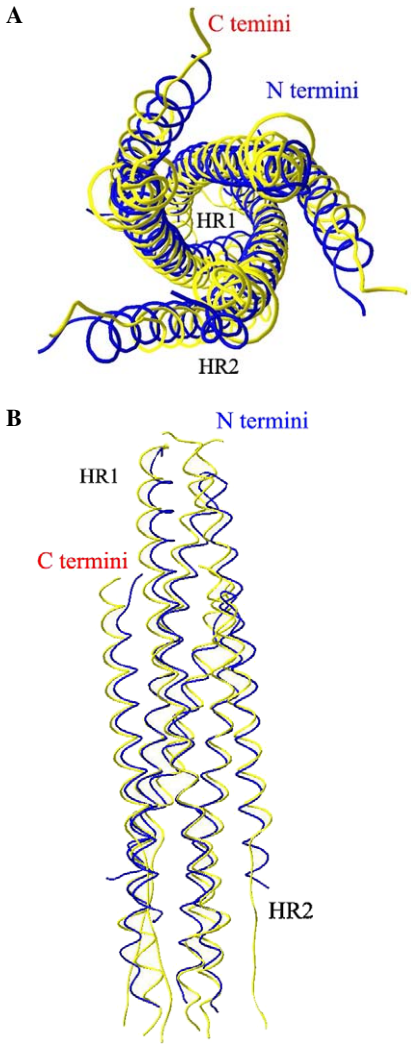

Fig. 3. Superposition of MuV fusion core (colored in blue) and SV5 F fusion core (colored in yellow). (A) Top view of the superposition. (B) Side view of the superposition. (For interpretation of the references to color in this figure legend, the reader is referred to the web version of this paper.)

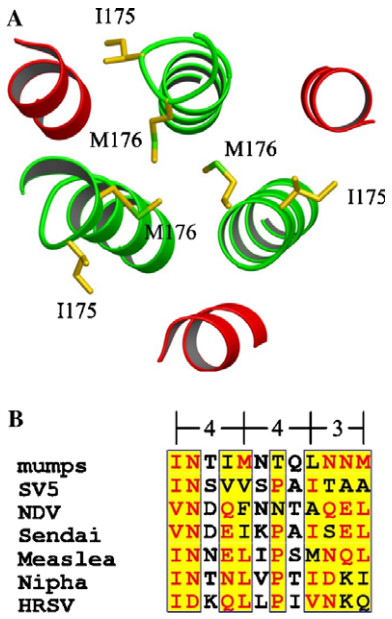

Fig. 4. Typical 3-4-4-4-3 spacing in MuV HR1 region. (A) Top view of part of helixes with I175 and M176 represented as stick mode, showing the I175 face to the outside of the central coiled-coil and M176 face to the center of the central coiled-coil. (B) Sequence alignment of MuV and other paramyxoviruses in the C terminus of HR1 region, indicating a typical 3-4-4-4-3 spacing in MuV HR1 regions similar with those in other paramyxoviruses.

Expectably, in MuV F structure, the residues in this region also form typical 4-4 spacing because residue I175 is at the d position and faces outside. We can consider that the skip pattern is conserved in paramyxovirus fusion proteins for executing fusion functions successfully.

Our structure studied here shows that HR2 of MuV fusion core has one additional extended region at the C terminus not observed in SV5 and HRSV C peptide. This additional extended region contains only four residues (SVNV). The extended chains can also be found at the N terminus of SV5 and HRSV HR2 regions. We can find a motif termed O–X–O in which O represents hydrophobic residues and X represents any residues, especially hydrophilic [17]. V^{477}-N^{478}-V^{479} in MuV F, L^{442}-S^{443}-I^{444} and L^{447}-D^{448}-I^{449} in SV5 F, L^{481}-V^{482}-F^{483} in HRSV F all belong to O–X–O motifs. The O–X–O pattern of hydrophobic residues is amphipathic when in an extended conformation but not in the context of α-helix. Therefore, this section of HR2 packs as an extended strand against the hydrophobic grooves between the HR1 helices. In these three structures, the distance between two hydrophobic residues in the O–X–O motifs is almost equal to 5.4 Å which is also the distance between the two adjacent turns in an α-helix. Thus, the two hydrophobic residues (O residues) could exactly pack against the grooves of the central coiled-coil formed by three HR1 helices just like residues at the a and d positions in normal heptad repeat regions of HR2. This compatibility of HR2 segments makes the fusion core more stable in solvent because most of the hydrophobic residues in HR2 regions are packed against the central coiled-coil and leave the hydrophilic residues faced the solvent. This pattern also explains why not all residues in HR2 of viral fusion proteins form α-helix and why HR1 peptides of these fusion proteins are highly conserved but HR2 peptides are always different in their three-dimensional conformations. Compatibilities of HR1 and HR2 segments we discussed here both indicate the basic rule for the formation of viral fusion core.

Conformational change

The structure of MuV fusion core adds to the repertoire of paramyxovirus six-helix bundle fusion core structures, of which only two are available at present, providing more structural information for the understanding of formation of fusion-active state of viral fusion proteins. The evident similarity between MuV F1 and well-studied viral fusion proteins like HIV gp41 and influenza HA, as well as previous biochemical anal-

ysis [20] indicates a similar mechanism of membrane fusion mediated by Mumps virus fusion protein. Similar to HIV gp41, MuV F1 likely has distinct conformational states, including the native state, the prehairpin intermediate, and fusion-active hairpin state [3]. The structure determined here likely corresponds to the fusion-active hairpin state of MuV F protein formed after several conformational changes, aligning cellular membrane and viral membrane juxtaposition which is followed by virus-cell membrane fusion.

Acknowledgments

This work was supported by a grant from the National Frontier Research Program (Project 973) of the Ministry of Science and Technology of the People's Republic of China (Grant No. G1999075602).

References

[1] J.S. Wolinsky, M.N. Waxham, Fields Virology, Raven Press, New York, 1990.
[2] K. Tanabayashi, K. Takeuchi, K. Okazaki, M. Hishiyama, A. Yamada, Expression of Mumps virus glycoproteins in mammalian cells from cloned cDNAs: both F and HN proteins are required for cell fusion, Virology 187 (1992) 801–804.
[3] P. Kuhn, J. Pieper, O. Kaminskaya, H.J. Eckert, R.E. Lechner, V. Shuvalov, G. Renger, Reaction pattern of Photosystem II: oxidative water cleavage and protein flexibility, Photosynth. Res. 84 (2005) 317–323.
[4] R.E. Dutch, T.S. Jardetzky, R.A. Lamb, Virus membrane fusion proteins: biological machines that undergo a metamorphosis, Biosci. Rep. 20 (2000) 597–612.
[5] D.C. Merz, A.C. Server, M.N. Waxham, J.S. Wolinsky, Biosynthesis of mumps virus F glycoprotein: non-fusing strains efficiently cleave the F glycoprotein precursor, J. Gen. Virol. 64 (Pt 7) (1983) 1457–1467.
[6] P.A. Bullough, F.M. Hughson, J.J. Skehel, D.C. Wiley, Structure of influenza haemagglutinin at the pH of membrane fusion, Nature 371 (1994) 37–43.
[7] M. Lu, S.C. Blacklow, P.S. Kim, A trimeric structural domain of the HIV-1 transmembrane glycoprotein, Nat. Struct. Biol. 2 (1995) 1075–1082.
[8] W. Weissenhorn, A. Dessen, S.C. Harrison, J.J. Skehel, D.C. Wiley, Atomic structure of the ectodomain from HIV-1 gp41, Nature 387 (1997) 426–430.
[9] S.C. Blacklow, M. Lu, P.S. Kim, A trimeric subdomain of the simian immunodeficiency virus envelope glycoprotein, Biochemistry 34 (1995) 14955–14962.
[10] W. Weissenhorn, S.A. Wharton, L.J. Calder, P.L. Earl, B. Moss, E. Aliprandis, J.J. Skehel, D.C. Wiley, The ectodomain of HIV-1 env subunit gp41 forms a soluble, alpha-helical, rod-like oligomer in the absence of gp120 and the N-terminal fusion peptide, Embo. J. 15 (1996) 1507–1514.
[11] D.C. Chan, D. Fass, J.M. Berger, P.S. Kim, Core structure of gp41 from the HIV envelope glycoprotein, Cell 89 (1997) 263–273.
[12] K. Tan, J. Liu, J. Wang, S. Shen, M. Lu, Atomic structure of a thermostable subdomain of HIV-1 gp41, Proc. Natl. Acad. Sci. USA 94 (1997) 12303–12308.
[13] M. Caffrey, M. Cai, J. Kaufman, S.J. Stahl, P.T. Wingfield, D.G. Covell, A.M. Gronenborn, G.M. Clore, Three-dimensional solution structure of the 44 kDa ectodomain of SIV gp41, EMBO J. 17 (1998) 4572–4584.
[14] W. Weissenhorn, A. Carfi, K.H. Lee, J.J. Skehel, D.C. Wiley, Crystal structure of the Ebola virus membrane fusion subunit, GP2, from the envelope glycoprotein ectodomain, Mol. Cell 2 (1998) 605–616.
[15] W. Weissenhorn, L.J. Calder, S.A. Wharton, J.J. Skehel, D.C. Wiley, The central structural feature of the membrane fusion protein subunit from the Ebola virus glycoprotein is a long triple-stranded coiled coil, Proc. Natl. Acad. Sci. USA 95 (1998) 6032–6036.
[16] K.A. Baker, R.E. Dutch, R.A. Lamb, T.S. Jardetzky, Structural basis for paramyxovirus-mediated membrane fusion, Mol. Cell 3 (1999) 309–319.
[17] Y. Xu, Y. Liu, Z. Lou, L. Qin, X. Li, Z. Bai, H. Pang, P. Tien, G.F. Gao, Z. Rao, Structural Basis for Coronavirus-mediated membrane fusion: crystal structure of mouse hepatitis virus spike protein fusion core, J. Biol. Chem. 279 (2004) 30514–30522.
[18] F.M. Hughson, Enveloped viruses: a common mode of membrane fusion? Curr. Biol. 7 (1997) R565–R569.
[19] D.C. Chan, P.S. Kim, HIV entry and its inhibition, Cell 93 (1998) 681–684.
[20] Y. Liu, J. Zhu, M.G. Feng, P. Tien, G.F. Gao, Six-helix bundle assembly and analysis of the central core of mumps virus fusion protein, Arch. Biochem. Biophys. 421 (2004) 143–148.
[21] Y. Xu, J. Zhu, Y. Liu, Z. Lou, F. Yuan, Y. Liu, D.K. Cole, L. Ni, N. Su, L. Qin, X. Li, Z. Bai, J.I. Bell, H. Pang, P. Tien, Z. Rao, G.F. Gao, Characterization of the heptad repeat regions, HR1 and HR2, and design of a fusion core structure model of the spike protein from severe acute respiratory syndrome (SARS) coronavirus, Biochemistry (2004).
[22] J. Zhu, G. Xiao, Y. Xu, F. Yuan, C. Zheng, Y. Liu, H. Yan, D.K. Cole, J.I. Bell, Z. Rao, P. Tien, G.F. Gao, Following the rule: formation of the six-helix bundle of the fusion core from severe acute respiratory syndrome coronavirus spike protein and identification of potent peptide inhibitors, Biochem. Biophys. Res. Commun. 319 (2004) 283–288.
[23] J. Zhu, P. Li, T. Wu, F. Gao, Y. Ding, C.W. Zhang, Z. Rao, G.F. Gao, P. Tien, Design and analysis of post-fusion six-helix bundle of heptad repeat regions from Newcastle disease virus F protein, Protein Eng. 16 (2003) 373–379.
[24] M. Yu, E. Wang, Y. Liu, D. Cao, N. Jin, C.W. Zhang, M. Bartlam, Z. Rao, P. Tien, G.F. Gao, Six-helix bundle assembly and characterization of heptad repeat regions from the F protein of Newcastle disease virus, J. Gen. Virol. 83 (2002) 623–629.
[25] Y. Xu, S. Gao, D.K. Cole, J. Zhu, N. Su, H. Wang, G.F. Gao, Z. Rao, Basis for fusion inhibition by peptides: analysis of the heptad repeat regions of the fusion proteins from Nipah and Hendra viruses, newly emergent zoonotic paramyxoviruses, Biochem. Biophys. Res. Commun. 315 (2004) 664–670.
[26] Z. Otwinowski, W. Minor, Macromolecular Crystallography, part A (Academic Press,1997), Methods Enzymol. 276 (1997) 307–326.
[27] A.T. Brunger, P.D. Adams, G.M. Clore, W.L. DeLano, P. Gros, R.W. Grosse-Kunstleve, J.S. Jiang, J. Kuszewski, M. Nilges, N.S. Pannu, R.J. Read, L.M. Rice, T. Simonson, G.L. Warren, Crystallography and NMR system: a new software suite for macromolecular structure determination, Acta Crystallogr. D Biol. Crystallogr. 54 (Pt 5) (1998) 905–921.
[28] T.A. Jones, J.Y. Zou, S.W. Cowan, Kjeldgaard, Improved methods for building protein models in electron density maps and the location of errors in these models, Acta. Crystallogr. A 47 (Pt 2) (1991) 110–119.
[29] R.A. Laskowski, M.W. MacArthur, D.S. Moss, J.M. Thornton, PROCHECK: a program to check the stereochemical quality of protein structures, J. Appl. Crystallogr. 26 (1993) 283–291.
[30] A. Nicholls, K.A. Sharp, B. Honig, Protein folding and association: insights from the interfacial and thermodynamic properties of hydrocarbons, Proteins 11 (1991) 281–296.
[31] N. Guex, M.C. Peitsch, SWISS-MODEL and the Swiss-PdbViewer: an environment for comparative protein modeling, Electrophoresis 18 (1997) 2714–2723.

[32] P.J. Kraulis, MOLSCRIPT: a program to produce both detailed and schematic plots of protein structures, J. Appl. Crystallogr. 24 (1991) 946–950.

[33] Y. Liu, Y. Xu, J. Zhu, B. Qiu, Z. Rao, G.F. Gao, P. Tien, Crystallization and preliminary X-ray diffraction analysis of central structure domains from Mumps virus F protein, Acta Crystallogr. F Biol. Crystallogr. 61 (2005) 855–857.

[34] X. Zhao, M. Singh, V.N. Malashkevich, P.S. Kim, Structural characterization of the human respiratory syncytial virus fusion protein core, Proc. Natl. Acad. Sci. USA 97 (2000) 14172–14177.

[35] M. Singh, B. Berger, P.S. Kim, LearnCoil-VMF: computational evidence for coiled-coil-like motifs in many viral membrane-fusion proteins, J. Mol. Biol. 290 (1999) 1031–1041.